Desalination and Water Treatment
www.deswater.com

doi:10.5004/dwt.2019.23460

139 (2019) 53–63
January

Comparative study between ceramsite media and quartz sand for the removal of methylene blue dye from aqueous solution in fixed-bed columns

Tianpeng Li[a,b,*], Tingting Sun[c], Tallal Bin Aftab[d], Jing Fan[b**], Ting Li[e]

[a]*College of City and Architecture Engineering, Zaozhuang University, Zaozhuang, Shandong 277160, China, email: tianpeng985@126.com (T.P. Li)*
[b]*School of Environment, Henan Normal University, Xinxiang, Henan 453007, China, email: fanjing@htu.cn (J. Fan)*
[c]*School of Basic Medical Science, Wenzhou Medical University, Wenzhou, Zhejiang 325035, China, email: ttsun@zju.edu.cn (T.T. Sun)*
[d]*College of Environment Science and Engineering, Donghua University, Shanghai 201620, China, email: tallal@live.com (T.B. Aftab)*
[e]*Zaozhuang Yuanheng Machinery Manufacturing Co., Ltd, Zaozhuang, Shandong 277000, China, email: yuanhengjx@163.com (T. Li)*

Received 17 June 2018; Accepted 12 November 2018

ABSTRACT

A comparative study for the removal of methylene blue (MB) dye from aqueous solution by ceramsite media (CM) and quartz sand (QS) in a two-stage fixed-bed column were investigated in this study. The results showed that under the optimum column experimental conditions of particle diameter was 0.5±0.2 mm, initial concentration was 5 mg/L, initial pH was 3, flow rate was 2 L/h and reaction temperature was 25°C, the breakthrough curve was much more smoothly when fixed-bed column packed with CM than that of packed with QS. The breakthrough and exhausted times of MB for CM were 620 and 1160 min, respectively, which were 41.94% and 46.55% higher than that for QS. The reasons are mainly due to the fact that CM, as a novel mesoporous material, has larger BET specific surface areas and higher porosity than that of QS. The linear regression analysis indicated that under the above optimal column conditions, the breakthrough curves of MB for both CM and QS were described with the A-B model ($R^2 = 0.977$) and Thomas model ($R^2 = 0.972$), respectively. In addition, the calculated maximum adsorption capacity of CM was 39.56 mg/g, about 69.77% higher than that of QS (11.96 mg/g). In conclusion, compared with QS, the fixed-bed column packed with CM exhibited much better adsorption performance with low initial concentration of MB dye, providing a prospective pathway for CM from solid wastes application in dye wastewater treatment.

Keywords: Ceramsite media; Quartz sand; Breakthrough curve; Fixed-bed column; Model analysis

1. Introduction

The dye wastewater, which exhibits a deep color, high concentrations of organics, slightly alkaline, multicomponent, high COD_{Cr} content, extremely low BOD to COD ratio and can potentially have high ammoniacal nitrogen content [1, 2]. The highly colored wastewater has become one of the most serious pollutants in water body, not only it causes scum formation, thermal impacts, color problems, and loss of esthetic beauty in the environment [3], but also its highly toxic to living organisms and is destructive for aquatic communities [4]. From an environmental perspective, the treatment of dye/dyeing containing wastewater is required prior to discharge, as it has attracted great attention from research and industrial application. To date, various physico/biochemical technologies have been developed to remove dyes from aqueous solution. Among these technologies, adsorption is an attractive method, due to its simple operation, cost-effective, energy-saving, highly efficient and environmental friendly [5–7].

Compared with batch adsorption experiment, the fixed-bed column adsorption process is more practical,

*Corresponding author.

owing to its more applicability to the industry [8,9]. Furthermore, the column setup has showed several remarkable advantages [10–12]: (I) The process is easy to monitor and operate, and it may be easily scaled up from laboratory to pilot unit; (II) It allows the contaminated water to be treated within a shorter time period; (III) It is more applicable to practical water treatment, with better effluent quality and high adsorption capacity. The performance of the column process greatly depends on the effectiveness of its design and operating conditions, which can provide more practical information for the wastewater treatment. Generally, due to the breakthrough phenomenon, the usual practice is either to use two or more columns in series and rotate them as they become exhausted [13].

The time for breakthrough appearance and the shape of the breakthrough curve are very important characteristics for determining the operation and dynamic response of a fixed-bed column. Numerous models, such as Bed Depth Service Time model (BDST model), Thomas model, Adams-Bohart model (A-B model), Yoon-Nelson model (Y-N model) and Convective-Dispersive model (C-D model), have been applied to analyze and explain the experimental data obtained from the laboratory scale fixed-bed columns, and also to predict the effect of various operational factors on the efficiency of adsorption process.

Recently, various fixed-bed column packing, such as activated carbon [14], triethylenetetramine functionalized microspheres [15], natural clay [16], Zeolite 4A [17], anthracite coal [18] and Auricularia auricula spent substrate [19], have been extensively studied during fixed-bed column adsorption process. However, there are still some major drawbacks in practical application for them. For instance, natural clay and zeolite are mineral resources, which do not meet with the requirements of sustainable development. Furthermore, active carbon has low selectivity, higher production cost, and difficult regeneration and reuse processes [20]. Hence, fixed-bed packing, with environmental friendly, easy preparation, excellent properties, great potential and low costs, is urgently needed.

Ceramsite, has proven to be a promising mesoporous material, with unique porous structure, high specific surface areas and large absorption capacity [21], due to these qualities it has attracted more attention in the field of water/wastewater treatment. It has been reported that a variety of raw materials, especially solid wastes, can be used to prepare ceramsite, due to similar mineral content [22,23]. Because of its excellent physical properties and lower heavy metal leaching toxicity, ceramsite or modified ceramsite or composite ceramsite, has been employed to remove heavy metals, organic pollutants and ammonium nitrogen from aqueous solution [24–27].

As a continuation of our previous research on, the objectives of the present work were to compare the removal effects of MB dye between CM and QS from aqueous solution in a two-stage fixed-bed column. Firstly, the as-obtained prepared CM and purchased QS, were pretreated and characterized; Secondly, by means of single factor test method, the effects of initial pH, flow rate and reaction temperature on the breakthrough curves of MB dye for the fixed-bed column packed with CM and QS were investigated and compared; Finally, several mathematical models, including Thomas, A-B and Y-N models, were employed to analyze the experimental data to predict the properties of fixed-bed packed with CM.

2. Materials and methods

2.1. Materials

The lab-made CM used in this work was obtained from dewatered sewage sludge, coal fly ash and river sediment, without using any natural resources. The CM was prepared by a high-temperature sintering process. Its physical properties are presented in Table 1. The preparation procedure, sintering high-temperature control process, physical-chemical properties and heavy metal leaching toxicity of CM were reported in our previous work [28,29]. In brief, the results confirmed that the novel CM is safe, reliable and can be further studied and applied as filter media, adsorbent or other media/material for water/wastewater treatment. Prior to the application, the CM was crushed down and sieved to a desired diameter. Consequently, it was washed several times with deionzied water, in order to remove the impurities in the inner pores and then it was dried in oven at 60°C for about 10 h.

The commercial QS (physical properties were illustrated in Table 1) was supplied by Zaozhuang Yuanheng Machinery Manufacturing Co., Ltd, Shandong Province, China. The QS was ground and to the required particle size. Before usage, it was washed several times with deionzied water to remove any impurities, and it was dried in oven at 60°C for about 10 h.

MB dye is a phenothiazne cation ($C_{16}H_{18}N_3SCl$; molecular weight 319.86). It is used in the study as a model for organic pollutant in general and basic dye in particular. The MB dye stock solution (500 mg/L) was prepared by dissolving accurately the weighed quantity of the dye in deionized water. The working solution was prepared thereafter by diluting the stock solution.

MB dye, HCl and NaOH were received from Sinopharm Chemical Reagent Co., Ltd, China. All the chemical reagents used in this research were of analytical grade and used as received without further purification. Deionized-water was employed in all experiments.

Table 1
Textural properties from N_2 adsorption-desorption isotherms and physical properties of samples

Samples	Specific surface area (m^2/g)	Total pore volume (m^3/g)	Mean pore diameter (nm)	Void fraction (%)	Piled density (g/cm^3)
CM	0.63	0.003	16.97	71.1	0.95
QS	0.31	0.0014	2.03	45	1.49

2.2. Column study

As noted previously [30], the CM and QS, with particle diameter of 0.5±0.2 mm, were chosen as the research objects, and the initial concentration of MB dye was 5 mg/L in this study. The schematic diagram of the two-stage fixed-bed column used in the research is shown in Fig. 1. To be specific, the column consisted of two cleaned parallel cylindrical glass tubes so that breakthrough in a single column will not significantly affect the effluent quality. The internal diameter, column height and valid volume of each tube were 7.5 cm, 50 cm and 2.2 × 10^3 cm^3, respectively. And a filter cloth was placed at the top and bottom of each tube, avoiding the penetration of packing. The column was packed with known quantity of fillings (CM or QS) to obtain a particular bed height. After that, the initial pH of the feed solution was adjusted with 0.1 mol/L HCl solution or 0.1 mol/L NaOH solution. The pH of initial solution was measured with a pH meter (Model: PHSJ-4F, INESA Scientific Instrument Co., Ltd, China). And then, it was fed into the column from the bottom of one tube and the effluent was discharged from the top of the other tube. The effluents were collected at different time intervals. The absorbance of MB dye was measured at its maximum wavelength of 664 nm by UV-Vis spectrophotometer (Model: UV-5500, Shanghai Metash instruments Co., Ltd, China) and subsequently, the MB concentrations were calculated according to the standard curve (see Fig. 2). All the column experiments were performed twice under the same conditions and an averaged value was used.

The breakthrough curve showed the performance of the fixed-bed column as it give clear sign of the breakthrough point, which can be defined as a point with respect to the time where the effluent concentration exceeds the maximum allowable discharge concentration for a specific water contaminant [31]. The MB dye adsorption breakthrough curve was obtained by plotting C_t/C_0 against t, where C_t (mg/L) is the effluent concentration, C_0 (mg/L) is the initial concentration and t (min) is the operating time. In this paper, the C_t reaches about 5% of the C_0 is the breakthrough point (C_t = 5% C_0), and the corresponding time is breakthrough time. The point where the C_t reaches 90% of the C_0 is called the "point of column exhaustion", C_t = 90% C_0, and the corresponding time is saturation time.

2.3. Mathematical models

(1) The Thomas model [32]

Thomas model is one of the most generally and widely used to describe the performance theory of the sorption process in fixed-bed column. This model assumes a second-order reversible reaction kinetics and the Langmuir isotherm. The linearized expression of Thomas model is given as follows:

$$\ln\left(\frac{C_t}{C_0 - C_t}\right) = K_{TH}C_0 t - \frac{K_{TH}q_0 m}{v} \quad (1)$$

where C_0 and C_t are the influent and effluent concentrations (mg/L), respectively; K_{TH} is the Thomas rate constant (mL/min/mg); q_0 is the maximum adsorption capacity (mg/g); m is the amount of adsorbent in the column (g); v is the volumetric flow rate (mL/min). The parameters K_{TH} and q_0 can be calculated from the linear plot of $ln[C_t/(C_0 - C_t)]$ against t.

(2) The Y-N model [33]

Y-N model is based on the assumption that the rate of decrease in the probability of adsorption for each adsorbate and the probability of adsorbate breakthrough on the adsorbent. The linearized Y-N model for a single component system can be expressed as:

$$\ln\left(\frac{C_t}{C_0 - C_t}\right) = K_{YN}t - \tau K_{YN} \quad (2)$$

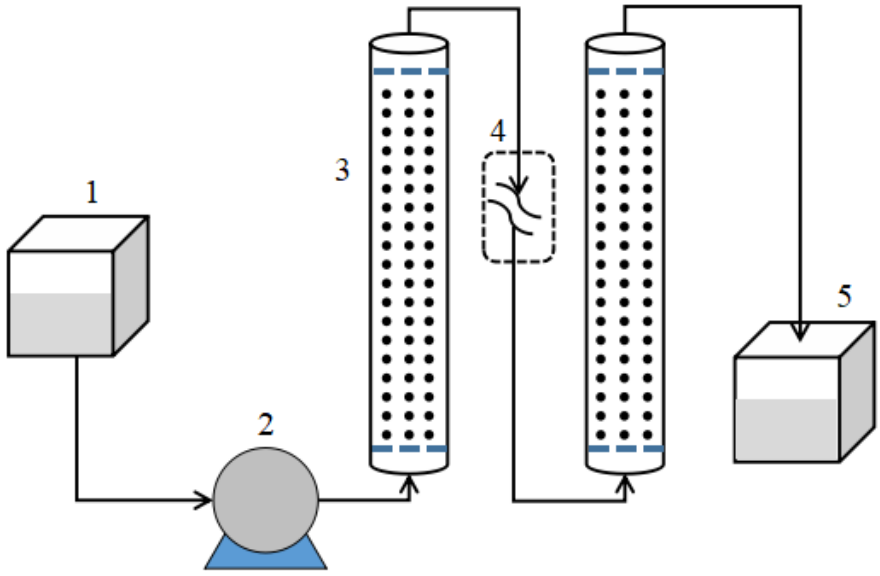

Fig. 1. Schematic diagram of two-stage fixed-bed adsorption column process (1-influent; 2-pump; 3-fixed-bed column; 4-space for an additional column; 5-effluent).

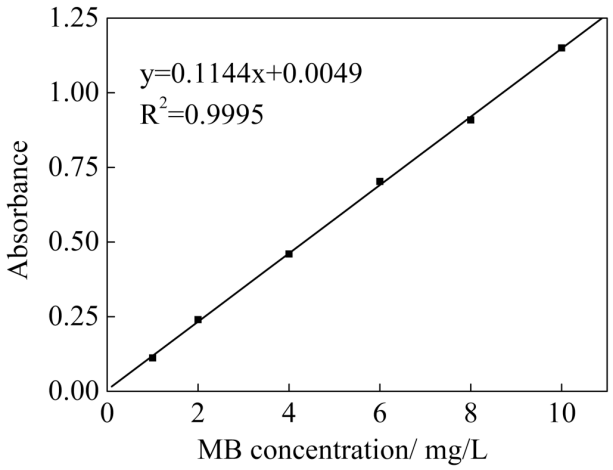

Fig. 2. The standard curve of MB concentration versus absorbance.

where C_0 and C_t are the influent and effluent concentrations (mg/L), respectively; K_{YN} is the rate constant (min^{-1}) and τ is the time required for 50% adsorbate breakthrough (min). A linear plot of $ln[C_t/(C_0 - C_t)]$ against t determined the values of K_{YN} and τ from the intercept and slope of the plot.

(3) The A-B model [34]

A-B model describes the relationship between C_t/C_0 and t in a continuous process. This model assumes that the equilibrium does not take place instantaneously and the adsorption rate is proportional to the residual capacity of the adsorbent and the concentration of the sorbing species. Its linear mathematical equation can be described as:

$$\ln\left(\frac{C_t}{C_0}\right) = K_{AB}C_0t - K_{AB}N_0\left(\frac{Z}{U_0}\right) \quad (3)$$

where C_0 and C_t are the influent and effluent concentrations (mg/L), respectively; K_{AB} is the kinetic constant (L/mg·min); N_0 is the saturation concentration (mg/L); Z is the bed depth of the fixed-bed column (cm) and U_0 is the superficial velocity (cm/min) defined as the ratio of the volumetric flow rate Q (mL/min) to the cross-seceration from the beginning to the end of breakthrough. The parameters K_{AB} and N_0 can be calculated from the linear plot of $ln(C_t/C_0)$ against t.

2.4. Characterization

The void fraction and piled density of samples were measured according to the China standard methods of Artificial Ceramsite Filter Material for Water Treatment (CJ/T 299-2008). A scanning electron microscope (SEM, Quanta-250, Fei Instrument, Czech) was used to observe the surface morphology of samples with an accelerating voltage of 13 kV. Before measurement, the surface of samples was sputtered with gold layer to improve the quality of the images. The Brunauer-Emmett-Teller (BET) specific surface area, S_{BET}, was calculated from N_2 adsorption and desorption measurements obtained using fully automatic specific and micro pore size analyzer (AUTOSORB-IQ2-MP, USA). Pore size distribution over the mesopore range was generated by the Barrett-Joyner-Halenda (BJH) analysis of the desorption branches, and the values for the average pore size were calculated.

3. Results and discussion

3.1. Effects of operating parameters

3.1.1. Effect of initial pH

The two-stage fixed-bed column experiments were carried out by varying the initial pH values from 3 to 11 (shown in Fig. 3A). Results showed that with increasing initial pH, the breakthrough curve became steeper and steeper, especially for Fig. 3a2. The breakthrough and saturation times of CM decreased from 620 to 520 min and 1160 to 980 min, respectively. In addition, as shown in Fig. 3a2, the breakthrough time decreased from 360 to 280 min with initial pH increased from 3 to 11, and the saturation time decreased from 620 to 500 min. These results indicated that the breakthrough and saturation times were the longest when initial pH was 3 for both CM and QS. Therefore, at lower initial pH, more time was required to reach the breakthrough and saturation point, which leading to lower MB concentration in effluent. Similar observations were also reported by other researchers [35].

Fascinatingly, Fig. 3A shows that under the column experimental conditions of initial pH = 3, inlet flow rate = 2 L/h and reaction temperature = 25°C, the breakthrough and saturation times of CM were 1.72 and 1.87 times longer than that of QS. It might be attributed to: (I) The surface of CM is coarse, poriferous and of lax structure (Fig. 4a), and the internal formation of numerous irregular holes, which is in favor of the adsorption of MB dye from water. On the contrary, the surface of QS is smooth and there are no porosity in its internal structure (Fig. 4b); (II) Table 1 reflects that the S_{BET}, total pore volume and mean pore diameter of CM from N_2 adsorption-desorption isotherms were 0.63 m^2/g, 0.03 m^3/g, 16.97 nm, respectively, which were much higher than that of QS, indicating that CM has better adsorption properties with higher $S_{BET,}$ larger pore volume and abundant pore size distribution.

Altogether, these results demonstrated that the initial pH of 3.0 offered anoptimum breakthrough curve, especially for CM. Hence, the subsequent experiments were carried out with this initial pH value.

3.1.2. Effect of flow rate

To optimize the conditions of the fixed-bed column for the treatment of wastewater on industrial scale, the flow rate is a very essential factor to study [36]. The effect of flow rates (in the range of 1–3 L/h) on the removal of MB dye from aqueous solution in the two-stage fixed-bed column are revealed by breakthrough curves in Fig. 3B. It was observed that within the investigated flow rates, lower flow rate resulted in smaller breakthrough curve gradient. This is due to slower transport of MB dye molecules

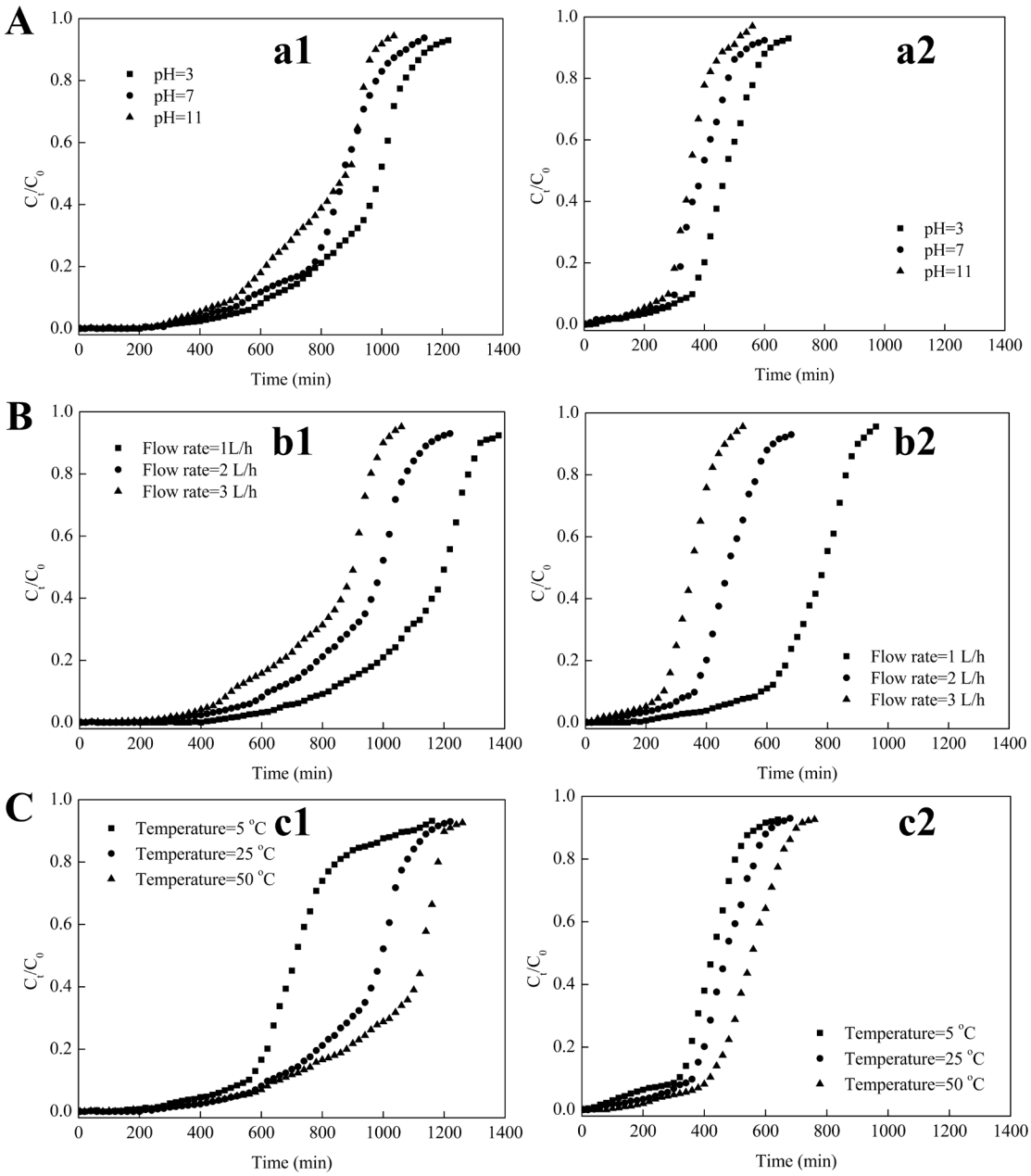

Fig. 3. Breakthrough curves for MB removal at different (A) initial pH (flow rate = 2 L/h, reaction temperature = 25°C; a1: CM; a2: QS), (B) flow rates (initial pH = 3, reaction temperature = 25°C; b1: CM; b2: QS) and (C) reaction temperatures (initial pH = 3, flow rate = 2 L/h; c1: CM; c2: QS).

into fillings, compared with a higher flow rate. Similar tendency has been found by other researchers [37,38]. Fig. 3b1 illustrates that compared with flow rate of 2 L/h, the breakthrough and saturation times increased by 12.12% and 24.39%, respectively, when flow rate was 1 L/h. Whereas, the breakthrough and saturation times decreased by 13.79% and 19.35%, respectively, when flow rate was 3 L/h. Fig. 3b2 also shows that the similar tendencies of the performance change.

It should be noted that when compared with QS, under the column experimental conditions of feed flow rate was 2 L/h, initial pH was 3 and reaction temperature was 25°C, the breakthrough and saturation times of CM prolonged to about 260 and 540 min, respectively. This phenomenon may be attributed to the contact time of MB dye molecule with CM or QS is very short at higher flow rate, which resulted in lower degree of adsorption and increasing in the effluent dye concentration. On the other hand, with the degree of turbulence and mixing increasing, the breakthrough occurs faster with increasing flow rate. As mentioned above, it can be deduced that the preferable inlet flow rate of the two-stage fixed-bed column is 2 L/h.

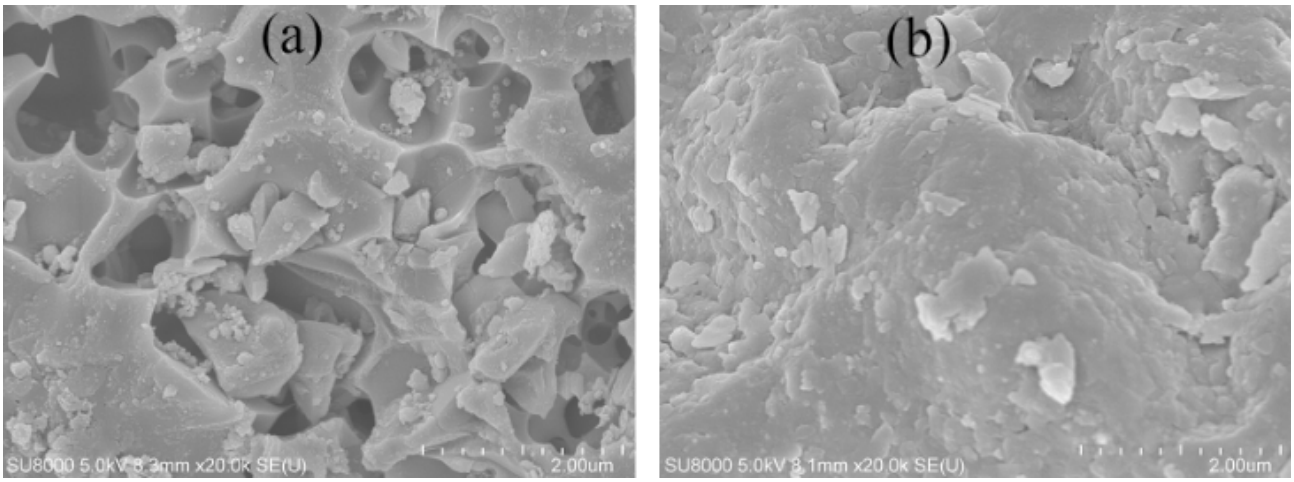

Fig. 4. SEM images of CM (a) and QS (b).

3.1.3. Effect of reaction temperature

The effect of reaction temperature at 5, 25 and 50±5°C on the breakthrough curve of MB dye in the two-stage fixed-bed column were assessed, as shown in Fig. 3C. Fig. 3c1 and Fig. 3c2 show that reaction temperature has little influence on the shape of breakthrough curve, especially for QS. However, more MB dye were removed from the influent when the reaction temperature increased from 5 to 50°C and the operating time was prolonged.

The breakthrough time of CM were 660, 620 and 560 min when the reaction temperature were set at 5, 25 and 50°C, respectively. The breakthrough time of QS were 420, 360 and 320 min at corresponding 5, 25 and 50°C, respectively. These results suggested that the fixed-bed column packed with CM needed more time to get its breakthrough point. Similarly, the saturation time of CM and QS were 1200, 1160 and 1100 min and 700, 620 and 580 min at the reaction temperature of 5, 25 and 50°C, respectively. This could be interpreted by the fact that high reaction temperature can promote the diffusion process of MB dye molecules from liquid phase to the surface of packing, leading to their adsorption or accumulation [26]. When the reaction temperature increased at 20°C (from 5 to 25°C), the breakthrough time of CM and QS were only extended about 60 and 40 min separately. On the contrary, when the reaction temperature increased at 25°C (from 25 to 50°C), the breakthrough time of CM and QS were only increased about 40 and 60 min. It can be concluded that reaction temperature had no significant effect on the column removal efficiency. It is undeniable that reaction temperature is an operation parameter, which can help compromise between operation costs and removal efficiency [39]. In this study, room temperature (25±5°C) was chosen as the optimal condition to investigate the effect of other factors on the two-stage fixed-bed column adsorption efficiency.

From the above discussion, it can be concluded that the shape of the breakthrough curve had a very close relationship to the column conditions, especially to the initial pH, the inlet flow rate, as well as reaction temperature. Under the column conditions of particle diameter = 0.5±0.2 mm, initial concentration = 5 mg/L, initial pH = 3, feed flow rate = 2 L/h and reaction temperature = 25°C, the breakthrough and exhausted times of CM were much longer than that of QS, and also with better column efficiency, low effluent MB concentration and lower operating cost.

3.2. Breakthrough curve modeling

For the purpose of industrial applications, designing prediction model is very important, especially for describing and analyzing the lab-scale column studies [40–42]. As aforementioned, several typical analytical models, including Thomas, A-B and Y-N models, were employed to fit the experimental data under different column experimental conditions. The aim was to identify the best model for predicting the adsorption behaviors of the two-stage fixed-bed column packed with CM and QS, respectively.

3.2.1. Thomas model

To better evaluate the removal performance of the two-stage fixed-bed column, the Thomas model was adopted to predict and analyze the relation between concentration and operating time of MB dye. The model parameters, K_{TH}, q_0 and correlation coefficient (R^2) were obtained using linear regression analysis according to Eq. (1). Fig. 5 and Table 2 indicate that the linear correlation of QS was better than that of CM under the investigated influence factors. According to the value of R^2 (greater than 0.95), the adsorption occurs followed by Langmuir-type isotherm, operation conditions isothermal and isobaric, no axial or radial dispersion and a second-order reversible kinetics, and the external and internal diffusion will not be the limiting step when the fixed-bed column packed with QS [43].

The K_{TH} values of CM increased with the initial pH and flow rate, as a result of high mass transfer rate. Nevertheless, it decreased from 1.70 to 1.22×10^{-3} mL/min/mg when reaction temperature increased. Likewise, the values of q_0 were reduced gradually along with the increasing of initial pH, while it slightly increased with the flow rate and reaction temperature. For QS, with the initial pH and flow rate increased, the value of K_{TH} increased, while the q_0 value had no significant

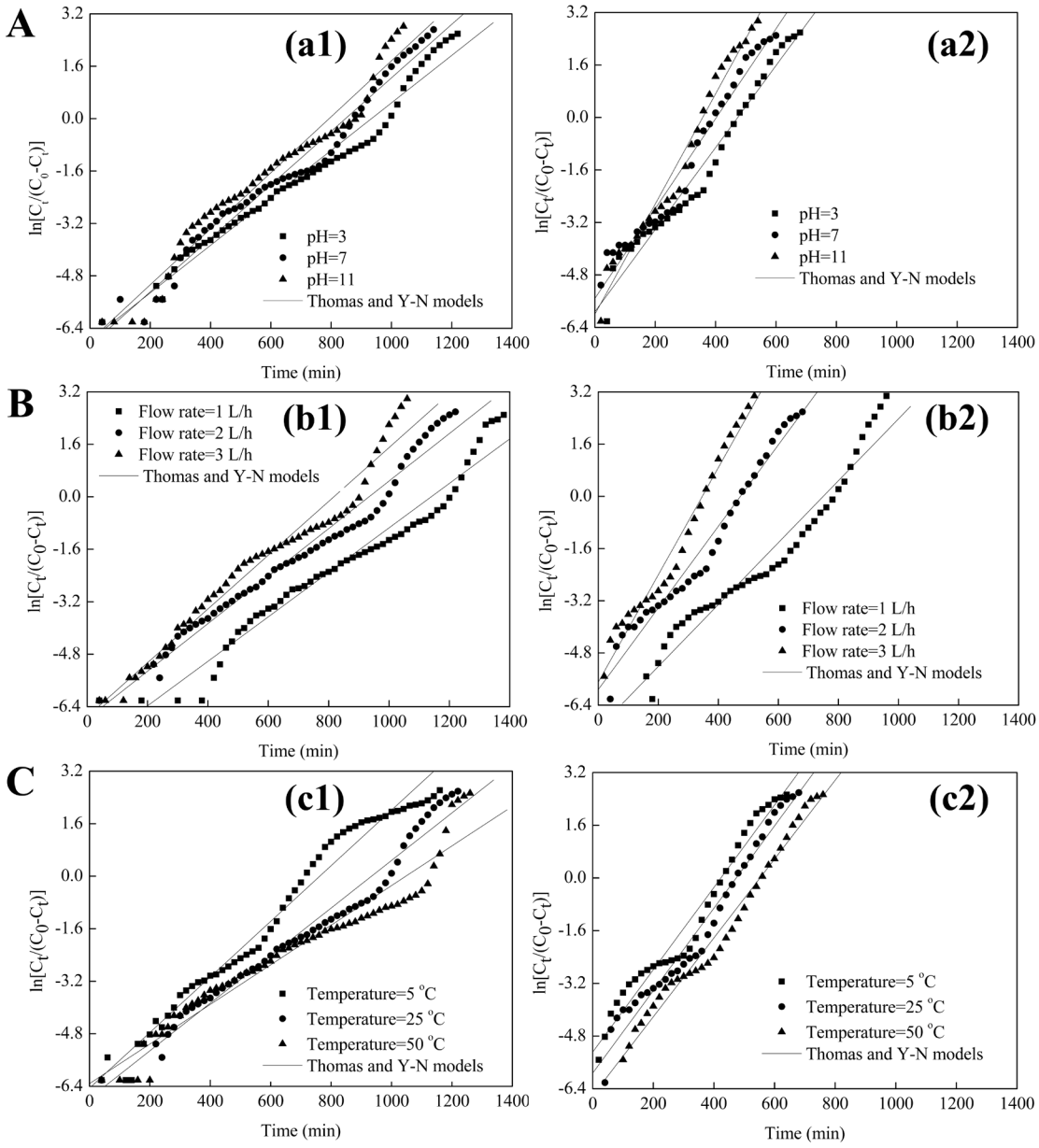

Fig. 5. Application of Thomas and Y-N models to the experimental data at at different (A) initial pH (flow rate = 2 L/h, reaction temperature = 25°C; a1: CM; a2: QS), (B) flow rates (initial pH = 3, reaction temperature = 25°C; b1: CM; b2: QS) and (C) reaction temperatures (initial pH = 3, flow rate = 2 L/h; c1: CM; c2: QS).

change. Besides, under the investigated column conditions, the q_0 value of CM is much higher than that of QS.

We also compared the calculated maximum adsorption capacity of MB dye with various adsorbent materials. Table 3 shows that the $q_{0\,cal}$ and adsorption capacity of CM employed in this work was comparable to other adsorbent materials, which indicated that CM shows a broad application prospect in dye wastewater treatment.

3.2.2. Y-N model

The Y-N model was used to interpret the removal performance of MB dye in the two-stage fixed-bed column packed with CM and QS, respectively. According to Fig. 3 and Eq. (2), the column parameters, included K_{YN}, τ and R^2, were analyzed by adopting the linear fitting. Fig. 5 and Table 2 illustrate that the tendency observed for both packing were very similar. For CM, the K_{YN} values increased gradually with the initial pH and flow rate, implying that the probability of adsorption for MB molecule decreases proportionately on the probabilities of the packing adsorption and breakthrough. By contrast, the value of τ increased significantly when the initial pH and inlet flow rate deceased. One possible explanation could be that the saturation of the packing occurs more rapidly [50]. Moreover, the value of τ increased with the reaction temperature, but the value of K_{YN} did not have much change.

Table 2
Parameters of (a) Thomas, (b) A-B and (c) Y-N models under different column experimental conditions

Packing	Initial pH	Flow rate (L/h)	Reaction temperature (°C)	Thomas model			Y-N model		A-B model		
				$K_{TH}\times10^{-3}$ mL/min/mg	q_0 mg/g	R^2	$K_{YN}\times10^{-3}$ min^{-1}	τ min	$K_{AB}\times10^{-3}$ L/mg·min	N_0 mg/L	R^2
CM	3	2	25	1.44	39.56	0.975	7.2	939.88	1.04	1873.88	0.977
	7	2	25	1.64	35.35	0.975	8.2	844.11	1.18	1701.05	0.951
	11	2	25	1.70	33.57	0.961	8.5	797.71	1.28	1574.17	0.923
	3	1	25	1.36	23.92	0.958	6.8	1136.90	1.04	1096.73	0.961
	3	3	25	1.64	51.59	0.970	8.2	817.26	1.24	2439.03	0.958
	3	2	5	1.70	31.97	0.976	8.5	759.52	1.16	1619.66	0.915
	3	2	50	1.20	44.32	0.939	6.0	1053.12	0.94	2052.59	0.951
QS	3	2	25	2.50	11.96	0.972	12.5	473.73	1.70	1008.27	0.952
	7	2	25	2.74	10.17	0.967	13.7	402.72	1.82	880.82	0.948
	11	2	25	3.36	9.02	0.977	16.8	357.02	2.14	796.03	0.937
	3	1	25	1.9	9.45	0.950	9.5	748.66	1.34	757.77	0.968
	3	3	25	3.28	13.15	0.973	16.4	347.26	2.12	1152.64	0.959
	3	2	5	2.50	10.67	0.967	12.5	422.6	1.62	939.77	0.943
	3	2	50	2.40	13.9	0.982	12.0	550.45	1.64	1143.94	0.969

Table 3
Comparison of the calculated maximum adsorption capacity ($q_{0\,Cal}$) for MB on different adsorbent materials

Adsorbent materials	$q_{0\,Cal}$ (mg/g)	Test type	References
CM	39.56	Column experiment	This work
QS	11.96	Column experiment	This work
Sand/single solution	5.31	Column experiment	[31]
MSM@PDA	14.58~84.53	Column experiment	[40]
αchitin nanoparticles(CNP)	Less than 9.45	Batch experiment	[44]
Poly nanospheres	Less than 23.91	Batch experiment	[45]
rGO-IO-60	39.00	Batch experiment	[46]
Carbon nanotubes	35.40	Batch experiment	[47]
Sawdust	48.79~87.30	Column experiment	[48]
Sludge carbon (SC-800)	30.2	Batch experiment	[49]

3.2.3. A-B model

The A-B model was employed to analyze the fixed-bed column breakthrough behaviors [51]. In this study, the predicted value of breakthrough curves were obtained from the A-B model (plotted in Fig. 6), and the K_{AB}, N_0 and R^2 values are presented in Table 2. We found that in the investigated influence factors, the R^2 (>0.95) valueof A-B model revealed better agreement with the experimental data of CM than that of QS. The K_{YN} value of CM had no significant change during the entire process of the experiment. The N_0 value of CM increased with the inlet flow rate and reaction temperature, suggesting that the removal efficiency of the column was dominated by external mass transfer. The K_{YN} and N_0 values of QS increased with the initial pH and flow rate, but no significantly change with the increasing of reaction temperature in the range of 5–50°C.

To ensure the accuracy of the model, the experimental data were characterized by the above mentioned three typical mathematical models. The plots exhibit linearity in the whole experiment which could be supported by high value of R^2. However, the A-B model has better relationship with the experimental data of CM than the other models, as shown by the statistical parameters determined from the experimental conditions. Moreover, the obtained experimental data of QS were in good agreement with Thomas model, as shown by the statistical parameters determined from the experimental conditions.

4. Conclusions

The present study compared the breakthrough behaviors for the removal of MB dye from aqueous solution by the two-stage fixed-bed column packed with CM and QS, respectively. The main conclusions derived from this study are as follows:

(1) The breakthrough point of CM shifted from left to right much slower than that of QS. Moreover, the

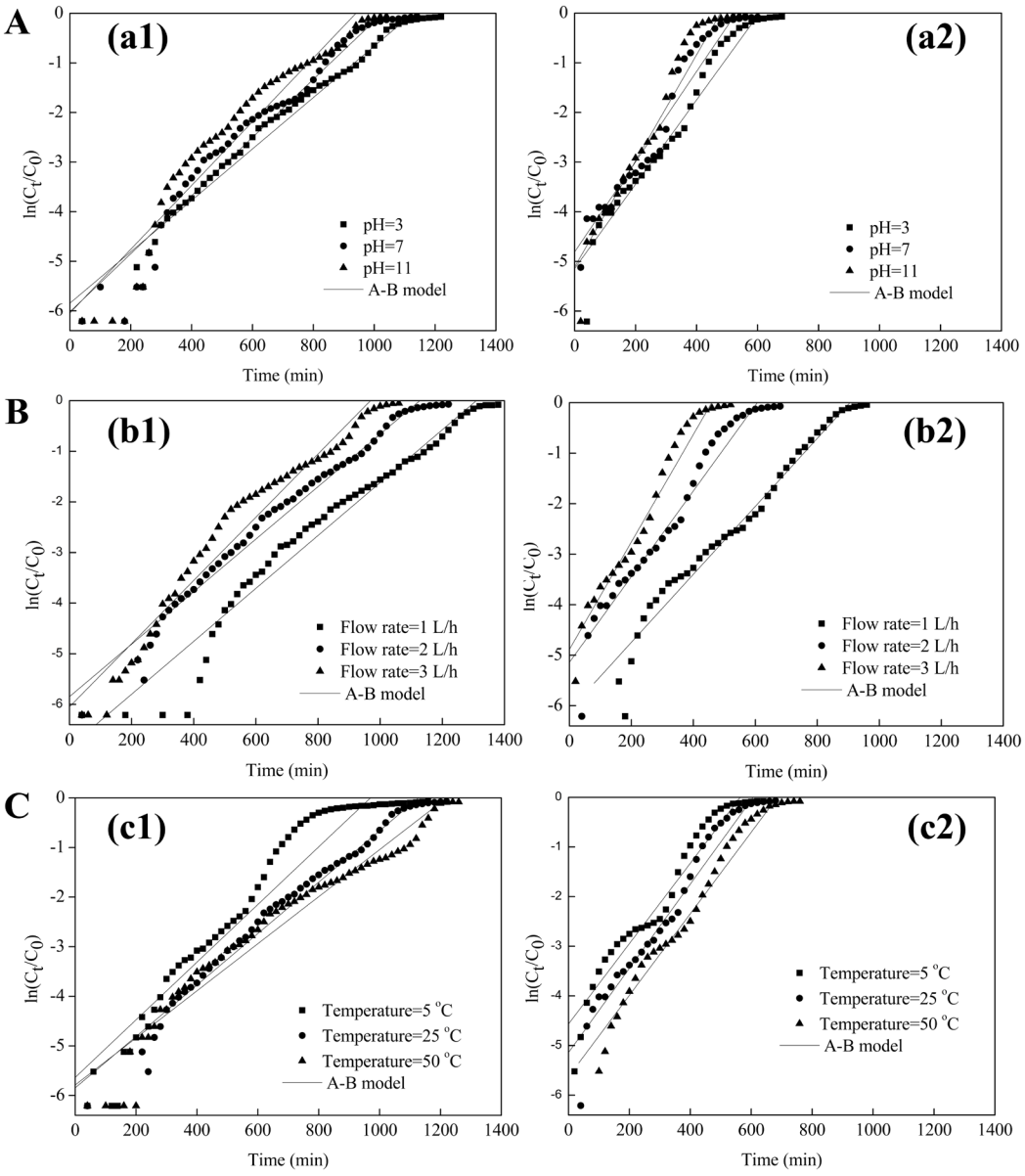

Fig. 6. Application of A-B model to the experimental data at at different (A) initial pH (flow rate = 2 L/h, reaction temperature = 25°C; a1: CM; a2: QS), (B) flow rates ((initial pH = 3, reaction temperature = 25°C; b1: CM; b2: QS) and (C) reaction temperatures (initial pH = 3, flow rate = 2 L/h; c1: CM; c2: QS).

breakthrough and saturation times of CM are 1.72 and 1.87 times higher than that of QS, suggesting that more time was required to reach the saturation point under the optimal column conditions for CM.

(2) The A-B model is the best model for mathematical description of MB dye removal in fixed-bed column packed with CM than the other selected models. The Thomas model is fitted well with the experimental results of fixed-bed column packed with QS. Besides, the maximum adsorption capacity of CM was improved by more than 70% than that of QS.

(3) CM, as a promising mesoporous material, obtained from solid wastes, has the advantage of high BET specific surface area and tampered pore structures, promising in application in the field of water treatment. Compared with the non-renewable natural resource of QS, the removal of MB dye wastewater by two-stage fixed-bed column packed with CM is more satisfactory.

Acknowledgments

This work was supported by the Natural Science Foundation Training Project of Shandong Province, China (No: ZR2018PEE026) and the Doctoral Scientific Research Foundation of Zaozhuang University (No: 2017BS01).

References

[1] J. Shi, B. Zhang, S. Liang, J. Li, Z. Wang, Simultaneous decolorization and desalination of dye wastewater through electrochemical process, Environ. Sci. Pollut. R., 4 (2018) 1–10.

[2] F. Feng, Z.L. Xu, X.H. Li, W.T. You, Y. Zhen, Advanced treatment of dyeing wastewater towards reuse by the combined Fenton oxidation and membrane bioreactor process, J. Environ. Sci., 22 (2010) 1657–1665.

[3] S.J. He, W.H. Sun, J.L. Wang, L.J. Chen, Y.X. Zhang, J. Yu, Enhancement of biodegradability of real textile and dyeing wastewater by electron beam irradiation, Radiat. Phys. Chem., 124 (2016) 203–207.

[4] Z.L. Yang, X.X. Liu, B.Y. Gao, S. Zhao, Y. Wang, Q.Y. Yue, Q. Li, Flocculation kinetics and floc characteristics of dye wastewater by polyferric chloride-poly-epichlorohydrin-dimethylamine composite flocculant, Sep. Purif. Technol., 118 (2013) 583–590.

[5] C. Zhu, J.N. Yun, Q. Wang, G. Yang, Adsorption of ion pairs onto graphene flakes and impacts of counterions during the adsorption processes, Appl. Surf. Sci., 435 (2018) 329–337.

[6] X.H. Wang, C.L. Jiang, B.X. Hou, Y.Y. Wang, C. Hao, J.B. Wu, Carbon composite lignin-based adsorbents for the adsorption of dyes, Chemosphere, 206 (2018) 587–596.

[7] Z.C. Yin, Y.L. Wang, K. Wang, C.B. Zhang, The adsorption behavior of hydroxypropyl guar gum onto quartz sand, J. Mol. Liq., 258 (2018) 10–17.

[8] M.J. Ahmed, B.H. Hameed, Removal of emerging pharmaceutical contaminants by adsorption in a fixed-bed column: A review, Ecotox. Environ. Safe., 149 (2018) 257–266.

[9] N.H. Shaidan, U. Eldemerdash, S. Awad, Removal of Ni(II) ions from aqueous solutions using fixed-bed ion exchange column technique, J. Taiwan Inst. Chem. E., 43 (2012) 40–45.

[10] A.L. Arim, K. Neves, M.J. Quina, L.M. Gando-Ferreira, Experimental and mathematical modelling of Cr(III) sorption in fixed-bed column using modified pine bark, J. Clean. Prod., 183 (2018) 272–281.

[11] S. Manna, P. Saha, D. Roy, B. Adhikari, P. Das, Fixed bed column study for water defluoridation using neem oil-phenolic resin treated plant bio-sorbent, J. Environ. Manage., 212 (2018) 424–432.

[12] N.E. Davila-Guzman, F.J. Cerino-Córdova, M. Loredo-Cancino, J.R. Rangel-Mendez, R. Gómez-González, E. Soto-Regalado, Studies of adsorption of heavy metals onto spent coffee ground: equilibrium, regeneration, and dynamic performance in a fixed-bed column, Int. J. Chem. Eng., 2 (2016) 1–11.

[13] P.W. Ye, Z.Q. Luan, J.C. Zhang, Z.L. Zhang, L. Ma, K. Li, L. Li, Y. Li, W.L. Cao, Study of adsorption kinetics of perfluoroisobutene on fixed bed activated carbon, J. Chem. Eng. Data, 53 (2008) 1262–1265.

[14] M.A.E.D. Franco, C.B.D. Carvalho, M.M. Bonetto, R.D.P. Soares, L.A. Féris, Diclofenac removal from water by adsorption using activated carbon in batch mode and fixed-bed column: Isotherms, thermodynamic study and breakthrough curves modeling, J. Clean. Prod., 181 (2018) 145–154.

[15] C.K. Liu, X.H. Luo, F. Wang, Z.K. Luo, X.X. Zhao, Copper ion adsorption behavior in a fixed-bed column filled by triethylenetetramine functionalized microspheres, Rare Metal Mat. Eng., 45 (2016) 180–183.

[16] D. Tiwari, Lalhmunsiama, S.I. Choi, S.M. Lee, Activated sericite: An efficient and effective natural clay material for attenuation of cesium from aquatic environment, Pedosphere, 24 (2014) 731–742.

[17] H.J. Liang, H. Gao, Q.Q. Kong, Z.X. Chen, Adsorption of tetrahydrofuran+water solution mixtures by Zeolite 4A in a fixed bed, J. Chem. Eng. Data, 52 (2007) 695–698.

[18] L.Z. Zou, J. Ai, H.Y. Fu, W. Chen, S.R. Zheng, Z.Y. Xu, D.Q. Zhu, Enhanced removal of sulfonamide antibiotics by KOH-activated anthracite coal: Batch and fixed-bed studies, Environ. Pollut., 211 (2016) 425–434.

[19] T.T. Zang, Z. Cheng, L. Lu, Y. Jin, X.H. Xu, W. Ding, J.J. Qu, Removal of Cr(VI) by modified and immobilized Auricularia auricula spent substrate in a fixed-bed column, Ecol. Eng., 99 (2017) 358–365.

[20] X.Q. Lin, G.X. Qi, S.L. Shi, L. Xiong, C. Huang, X.F. Chen, H.L. Li, X.D. Chen, Estimation of fixed-bed column parameters and mathematical modeling of breakthrough behaviors for adsorption of levulinic acid from aqueous solution using SY-01 resin, Sep. Purif. Technol., 174 (2017) 222–231.

[21] M.T. Sun, S.F. Fu,S. He, X.L. Fan, R.B. Guo, Effects of ceramsite on methane and hydrogen sulphide productions from macroalgae biomass, J. Cent. South Univ., 25 (2018) 1076–1083.

[22] J.L. Wang, Y.L. Zhao, P.P. Zhang, L.Q. Yang, H.A. Xu, G.P. Xi, Adsorption characteristics of a novel ceramsite for heavy metal removal from stormwater runoff, Chinese J. Chem. Eng., 26 (2018) 96–103.

[23] T.P. Li, T.T. Sun, T.B. Aftab, D.X. Li, Photocatalytic degradation of methylene blue in aqueous solution using ceramsite coated with micro-Cu_2O under visible-light irradiation, Korean J. Chem. Eng., 34 (2017) 1199–1207.

[24] L.L. Zhou, G.L. Zhang, M. Wang, D.F. Wang, D.Q. Cai, Z.Y. Wu, Efficient removal of hexavalent chromium from water and soil using magnetic ceramsite coated by functionalized nano carbon spheres, Chem. Eng. J., 334 (2018) 400–409.

[25] M. Wang, G.L. Zhang, T. Pang, D.Q. Cai, Z.Y. Wu, Removal of anthracemethanol from soil through a magnetic system assisted by ceramsite coated with nanoflower-structured carbon and preparation for its engineering application, Chem. Eng. J., 328 (2017) 748–758.

[26] T.P. Li, T.T. Sun, T.B. Aftab, D.X. Li, Adsorption isotherms, kinetics and thermodynamics of ammonium nitrogen from aqueous solutions using modified ceramsite and it's regeneration performance, Desal. Water Treat., 90 (2017) 196–205.

[27] S. Qiu, X. Huang, S.W. Xu, F. Ma, The antibacterial activity of ceramsite coated by silver nanoparticles in micropore, Appl. Biochem. Biotechnol., 176 (2015) 267–276.

[28] T.P. Li, T.T. Sun, D.X. Li, Preparation, sintering behavior and expansion performance of ceramsite filter media from dewatered sewage sludge, coal fly ash and river sediment, J. Mater. Cycles Waste Manage., 20 (2018) 71–79.

[29] T.P. Li, T.T. Sun, T.B. Aftab, D.X. Li, X.L. Lin, Y.L. Li, Preparation and physical properties of ceramsite filter media for water treatment obtained from municipal solid wastes, J. Donghua Univ. (English Edition), 34 (2017) 39–44.

[30] T.P. Li, T.T. Sun, D.X. Li, Removal of methylene blue from aqueous solution by ceramsite filter media combined with high temperature calcination for regeneration, Desal. Water Treat., 59 (2017) 220–229.

[31] J.L. Gong, Y.L. Zhang, Y. Jiang, G.M. Zeng, Z.H. Cui, K. Liu, C.H. Deng, Q.Y. Niu, J.H. Deng, S.Y. Huan, Continuous adsorption of Pb (II) and methylene blue by engineered graphite oxide coated sand in fixed-bed column, Appl. Surf. Sci., 330 (2015) 148–157.

[32] R. Han, Y. Wang, W. Zou, Y. Wang, J. Shi, Comparison of linear and nonlinear analysis in estimating the Thomas model parameters for methylene blue adsorption onto natural zeolite in fixed-bed column, J. Hazard. Mater., 145 (2007) 331–335.

[33] S. Mohan, D.K. Singh, V. Kumar, S.H. Hasan, Effective removal of Fluoride ions by rGO/ZrO_2 nanocomposite from aqueous solution: fixed bed column adsorption modeling and its adsorption mechanism, J. Fluorine Chem., 194 (2017) 40–50.

[34] N.E. Messaoudi, M.E. Khomri, A. Dbik, S. Bentahar, A. Lacherai, B. Bakiz, Biosorption of congo red in a fixed-bed column from aqueous solution using jujube shell: experimental and mathematical modeling, J. Environ. Chem. Eng., 4 (2016) 3848–3855.

[35] H.Y. Shu, M.C. Chang, J.J. Liu, Cation resin fixed-bed column for the recovery of valuable THAM reagent from the wastewater, Process Safe. Environ., 104 (2016) 571–586.

[36] M. Nishil, G. Nathan, W.H. Ambrose, R.M. Berry, T.K. Chiu, Continuous flow adsorption of methylene blue by cellulose nanocrystal-alginate hydrogel beads in fixed bed columns, Carbohyd. Polym., 136 (2016) 1194–1202.

[37] S.H. Chen, Q.Y. Yue, B.Y. Gao, Q. Li, X. Xu, K.F. Fu, Adsorption of hexavalent chromium from aqueous solution by modified corn stalk: A fixed-bed column study, Bioresource Technol., 113 (2012) 114–120.

[38] N. Sivarajasekar, K. Balasubramani, N. Mohanraj, J.P. Maran, S. Sivamani, P.A. Koya, V. Karthik, Fixed-bed adsorption of atrazine onto microwave irradiated Aegle marmelos Correa fruit shell: Statistical optimization, process design and breakthrough modeling, J. Mol. Liq., 241 (2017) 823–830.
[39] A. Ruiz-Martínez, J. Serralta, A. Seco, J. Ferrer, Effect of temperature on ammonium removal in Scenedesmus sp., Biores. Technol., 191 (2015) 346–349.
[40] M. Riazi, A.R. Keshtkarb, M.A. Moosavian, Biosorption of Th(IV) in a fixed-bed column by Ca-pretreated Cystoseiraindica, J. Environ. Chem. Eng., 4 (2016) 1890–1898.
[41] T. Ataei-Germi, A. Nematollahzadeh, Bimodal porous silica microspheres decorated with polydopamine nano-particles for the adsorption of methylene blue in fixed-bed columns, J. Colloid Interf. Sci., 470 (2016) 172–182.
[42] Z. Xu, J.G. Cai, B.C. Pan, Mathematically modeling fixed-bed adsorption in aqueous systems, J. Zhejiang Univ.-Sci. A (Appl. Phys. and Eng.), 14 (2013) 155–176.
[43] N. Rahman, M.F. Khan, Nitrate removal using poly-o-toluidine zirconium(IV) ethylenediamine as adsorbent: Batch and fixed-bed column adsorption modelling, J. Water Process Eng., 9 (2016) 254–266.
[44] S. Dhananasekaran, R. Palanivel, S. Pappu, Adsorption of methylene blue, bromophenol blue, and coomassie brilliant blue by a-chitin nanoparticles, J. Adv. Res., 7 (2016) 113–124.
[45] Z.H. Chen, J.W. Fu, M.H. Wang, X.Z. Wang, J.A. Zhang, Q. Xu, Adsorption of cationic dye (methylene blue) from aqueous solution using poly (cyclotriphosphazene-co-4,4-sulfonyldiphenol) nanospheres, Appl. Surf. Sci., 289 (2014) 495–501.
[46] F. Sharif, L.R. Gagnon, S. Mulmi, E.P.L. Roberts, Electrochemical regeneration of a reduced graphene oxide/magnetite composite adsorbent loaded with methylene blue, Water Res., 114 (2017) 237–245.
[47] Y.J. Yao, F.F. Xu, M. Chen, Z.X. Xu, Z.W. Zhu, Adsorption behavior of methylene blue on carbon nanotubes, Biores. Technol., 101 (2010) 3040–3046.
[48] S. Dardouri, J. Sghaier, A comparative study of adsorption and regeneration with different agricultural wastes as adsorbents for the removal of methylene blue from aqueous solution, Chinese J. Chem. Eng., 25 (2017) 1282–1287.
[49] I. Sierra, U. Iriarte-Velasco, M. Gamero, A.T. Aguayo, Upgrading of sewage sludge by demineralization and physical activation with CO_2: Application for methylene blue and phenol removal, Micropor. Mesopor. Mat., 250 (2017) 88–99.
[50] G. Nazari, H. Abolghasemi, M. Esmaieli, E.S. Pouya, Aqueous phase adsorption of cephalexin by walnut shell-based activated carbon: A fixed-bed column study, Appl. Surf. Sci., 375 (2016) 144–153.
[51] T.M. Darweesh, M.J. Ahmed, Adsorption of ciprofloxacin and norfloxacin from aqueous solution onto granular activated carbon in fixed bed column, Ecotox. Environ. Safe., 138 (2017) 139–145.